Science Advances

AAAS

advances.sciencemag.org/cgi/content/full/4/4/eaar2632/DC1

# Supplementary Materials for

## The delivery of water by impacts from planetary accretion to present

R. Terik Daly and Peter H. Schultz

Published 25 April 2018, *Sci. Adv.* **4**, eaar2632 (2018)
DOI: 10.1126/sciadv.aar2632

**This PDF file includes:**

**Supplementary Text**

Detailed description of alternative sources of water

In addition to the antigorite projectile, impact materials could incorporate water from the heat-treated pumice target, from the residual atmospheric water vapor in the impact chamber, from a monolayer of water molecules adsorbed onto the pumice, or during the time that elapsed between the experiments and TG analyses.

*Option 1: Target-derived water.* As described in the Results section, the heat-treated pumice contained 0.13 wt.% OH + $H_2O$. To compensate for this water, 0.13 wt.% was subtracted from the weight loss of each sample prior to calculating water content. For example, if a sample lost 1% of its mass, only 0.87% was used in our calculations of the amount of water derived from the projectile.

*Option 2: Atmospheric water vapor in the impact chamber.* During these experiments the pressure in the impact chamber was between 5.0 and 6.3 x $10^{-4}$ atm. Impact products may have trapped some of the residual water vapor in the chamber. On the warmest day that the experiments were conducted, the average temperature was 21.7°C (71°F). The maximum relative humidity was 86%. The dew point was 12.8°C (55°F). The atmospheric pressure was 29.98 inches of Hg (data for 13 July 2016 at the Moffett Federal Airfield; accessed via *wunderground.com*). Hence, the absolute humidity was 16 g $m^{-3}$. The impact chamber has a volume of about 59 $m^3$. Prior to pumping, the air in the impact chamber would have contained 944 g of water vapor. Once the chamber was pumped down to 5 x $10^{-4}$ atm, however, the chamber only contained ~19 mg of water vapor, most of which would be adsorbed on the interior surfaces of the chamber. Furthermore, the impact products only interacted with a tiny volume (<1%) of the residual gas in the impact chamber. By comparison, the antigorite projectiles contained ~60 mg of OH. Thus, residual water vapor cannot significantly contribute to the water content of the breccias or glasses.

*Option 3: Adsorbed monolayer of water.* Another possibility is that a monolayer of adsorbed water coated pumice grains at the time of experiments. Such water might have been trapped along grain boundaries during shock lithification and contribute to the unusually high water contents of the breccias. However, simple calculations show that contribution is also negligible.

In order to calculate the amount of adsorbed water, the reactive surface area of the pumice must be known. Although the reactive surface area of the sieved airfall pumice has not been directly measured, it is likely similar to that of volcanic ash. Delmelle et al. (*48*) reported data for six samples of volcanic ash with particles <100 μm. The pumice particles used in this study are <106 μm. Hence, the measurements are relevant to the pumice particles used in the present study. The specific surface areas of the samples measured by Delmelle et al. (*48*) ranged from 1.1 to 2.1 $m^2$ $g^{-1}$. The density of surface OH groups on amorphous silica is 4.9 OH per square nanometer (*21*). Recovered breccias contain an average of 0.56 g of pumice. If the specific surface area of the pumice were 2.1 $m^2$ $g^{-1}$ and all reactive sites were hydroxylated, then the pumice in the breccias would contain ~5 x $10^{18}$ surface silanol groups. If every silanol were hydrogen bonded to a water molecule, then the total mass of water in the silanol and $H_2O$

monolayer would be 0.3 mg, an amount equivalent to only ~0.05% of the mass of pumice in the breccias. If the specific surface area of the pumice were 1.1 $m^2 g^{-1}$, then the total mass of adsorbed water would be ~0.2 mg (under the same assumptions), an amount equivalent to ~0.04% of the mass of pumice in the breccias. Given that breccias lost 2.0 to 2.7 wt.% during TGA, a pre-impact adsorbed monolayer on pumice particles is, at most, a very minor component of the water budget of breccias or glasses.

Alternatively, breccias might have trapped water desorbed from pumice particles during impact. Once released, this water vapor (derived from the target) might have be trapped in the breccias, analogous to the process proposed for water vapor derived from the projectile. The temperature required to remove an adsorbed monolayer of water is ~190°C for amorphous silica (*21*). The pumice exposed to these conditions is located beneath the point of impact and comes from a region roughly cylindrical in shape. The cylindrical region is about three projectile radii high (~9.5 mm) and three projectile radii in diameter. The density of the pumice is ~1.2 g $cm^{-3}$. Therefore, this cylindrical region contains about 0.8 g of pumice. Using the same specific surface areas and assumptions as in the previous paragraph, an adsorbed monolayer could contribute between 0.2 and 0.5 mg of water. This amount is, at most, only 0.8% of the mass of water in the projectile. Hence, an adsorbed monolayer on pumice particles prior to impact cannot account for the high water contents of breccias and glasses.

*Option 4: Post-impact addition of water.* The fourth option is that breccias adsorbed water from their environment between the time of the experiments and the time of the TG analyses. Most adsorbed water should be removed by 100°C, yet the masses of the samples changed very little below 100°C: the breccias only lost 0.06 to 0.12 wt.% below 100°C (in contrast to the ~2 wt.% lost between 100 and 850°C). Furthermore, the antigorite equivalent calculations only considered mass losses between 190 and 850°C. Hence, post-impact adsorption or absorption cannot account for the high water contents of the breccias and glasses.

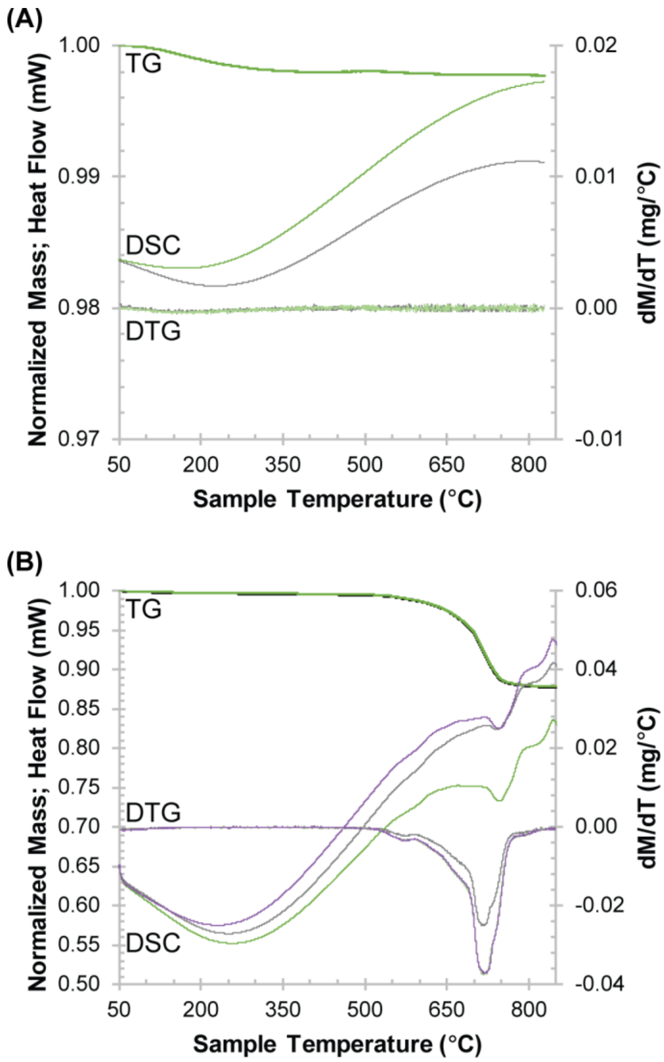


**fig. S1. TG data for the target and projectile.** Thermogravimetric (TG), derivative thermogravimetric (DTG), and differential scanning calorimetry (DSC) profiles for (**A**) the heat-treated pumice target and (**B**) antigorite projectiles. The y-axis at left is for both TG and DSC profiles. For pumice, the DSC data have been divided by 10,000 and offset by +0.96 so they can plot on the same axis as the TG data. For antigorite, the DSC data have been divided by 300 and offset by +0.3 for the same reason. The y-axis at right is for the DTG data.

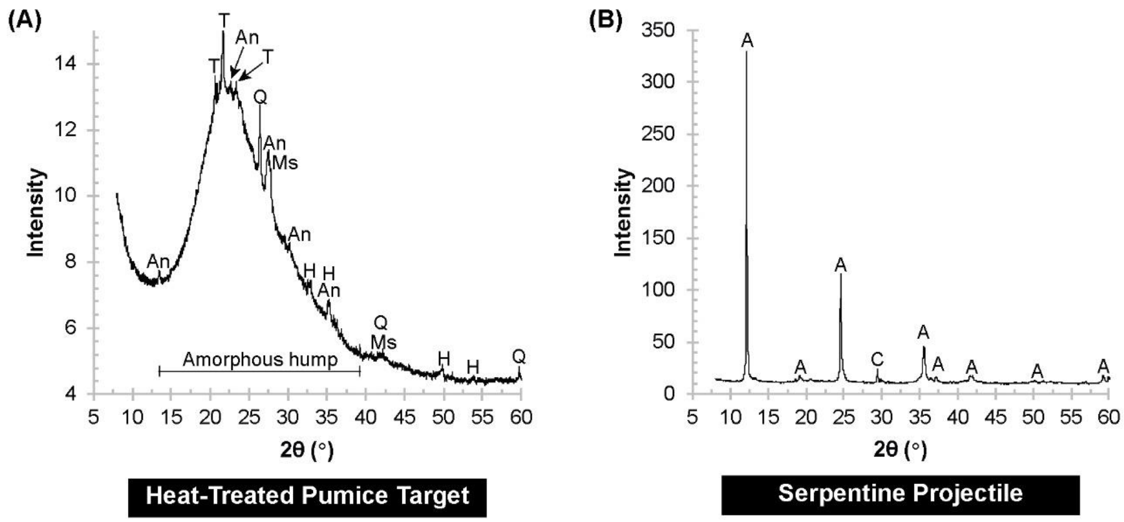


**fig. S2. XRD data for the target and projectile.** X-ray diffraction patterns for (**A**) the heat-treated pumice target and (**B**) the antigorite projectile. The heat-treated pumice is predominately glass, with minor anorthite (An), tridymite (T), quartz (Q), muscovite (Ms), and hematite (H). The antigorite projectile is nearly pure antigorite (A) with only a minor amount of calcite (C).

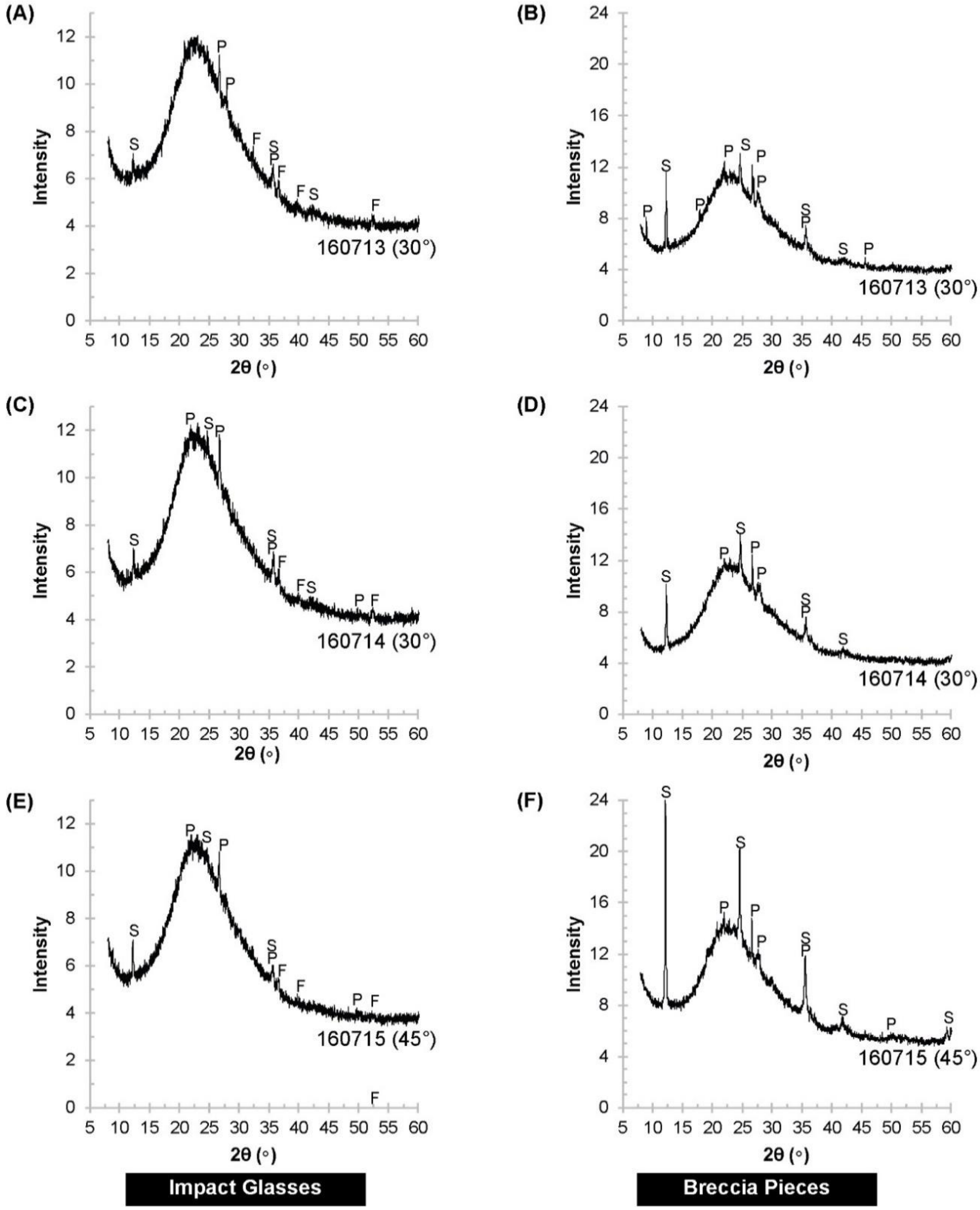


**fig. S3. XRD patterns for impact glasses and breccias.** (**A**) and (**B**) show the patterns for impact glasses and breccias from experiment 160713, respectively. (**C**) and (**D**) show the patterns for impact glasses and breccias from experiment 160714, respectively. (**E**) and (**F**) show the patterns for impact glasses and breccias from experiment 160715, respectively. Peaks labeled "S" are due to the serpentine (antigorite) projectile, while peaks labeled "P" are from the pumice target. Forsterite (F) is a decomposition product of antigorite.

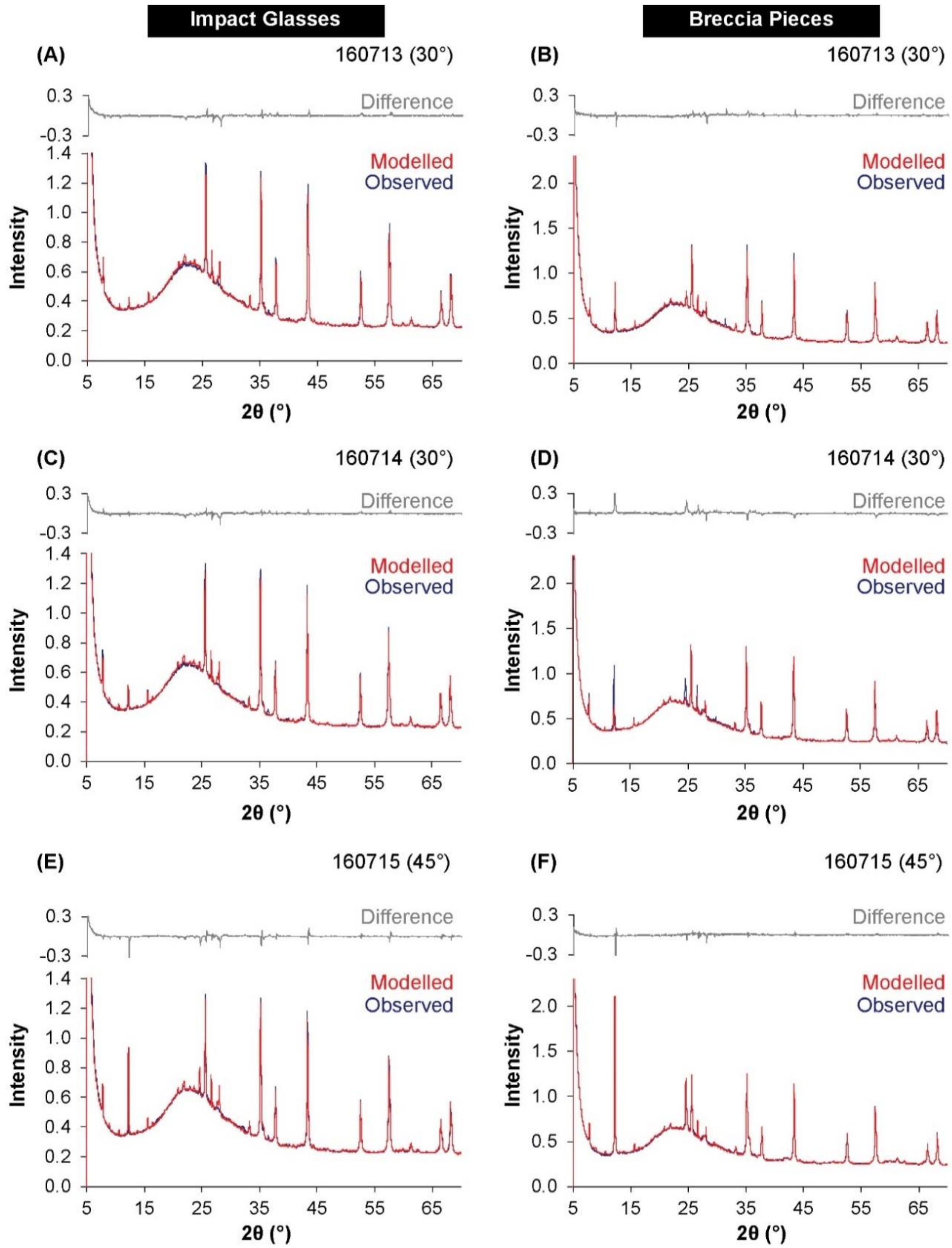


**fig. S4. Comparison between observed and modeled XRD patterns.** Each panel shows the observed pattern in blue and the model patterns produced by FULLPAT in red. Small gray graphs show the difference between the observed and modeled patterns. (**A**) and (**B**) show the patterns for glasses and breccias from experiment 160713, respectively. (**C**) and (**D**) show the patterns for glasses and breccias from experiment 160714, respectively. (**E**) and (**F**) show the patterns for glasses and breccias from experiment 160715, respectively.

**table S1. Summary of experiments.**

| Exp. number | Impact angle | Target | Projectile | Projectile diameter | Weight (g) | Velocity (km $s^{-1}$) | Impact glasses recovered (g) | Breccia pieces covered (g) | Antigorite relics recovered (g) | Total recovered mass (g) |
|---|---|---|---|---|---|---|---|---|---|---|
| 160713 | 30° | Heat-treated pumice | Antigorite | 6.35 mm | 0.4894 | 5.00 | 0.4221 | 0.5686 | 0.0117 | 1.0023 |
| 160714 | 30° | Heat-treated pumice | Antigorite | 6.35 mm | 0.5152 | 5.12 | 0.5095 | 0.6501 | 0.0161 | 1.1758 |
| 160715 | 45° | Heat-treated pumice | Antigorite | 6.35 mm | 0.5090 | 5.12 | 0.4717 | 0.5754 | 0.0400 | 1.0870 |

**table S2. Composition of antigorite relics measured by EMP (wt %).**

| Experiment ID | Spot | MgO | $FeO_T$ | CaO | $Al_2O_3$ | $SiO_2$ | Total |
|---|---|---|---|---|---|---|---|
| 160713 (30°) | 1 | 36.93 | 5.03 | 0.12 | 2.38 | 42.70 | 87.16 |
| | 2 | 36.94 | 5.31 | 0.09 | 2.80 | 42.50 | 87.64 |
| | 3 | 37.14 | 5.35 | 0.03 | 2.60 | 42.51 | 87.63 |
| | 4 | 37.25 | 5.33 | 0.00 | 2.77 | 42.73 | 88.08 |
| | 5 | 36.88 | 5.29 | 0.03 | 2.88 | 42.36 | 87.44 |
| | 6 | 36.68 | 5.27 | 0.00 | 2.41 | 42.68 | 87.04 |
| | 7 | 37.13 | 5.08 | 0.01 | 2.24 | 43.03 | 87.49 |
| 160714 (30°) | 1 | 37.63 | 5.04 | 0.00 | 1.86 | 43.60 | 88.13 |
| | 2 | 37.25 | 5.04 | 0.00 | 2.15 | 43.16 | 87.60 |
| | 3 | 36.95 | 4.90 | 0.00 | 2.04 | 43.30 | 87.20 |
| | 4 | 36.85 | 5.21 | 0.00 | 2.36 | 42.99 | 87.41 |
| | 5 | 37.10 | 5.06 | 0.00 | 2.27 | 43.35 | 87.77 |
| | 6 | 36.85 | 5.14 | 0.01 | 2.32 | 42.84 | 87.16 |
| 160715 (45°) | 1 | 36.43 | 5.27 | 0.02 | 2.69 | 41.95 | 86.36 |
| | 2 | 32.87 | 5.62 | 0.02 | 11.39 | 35.58 | 85.48 |
| | 3 | 33.08 | 5.39 | 0.03 | 12.36 | 35.35 | 86.21 |
| | 4 | 36.44 | 5.14 | 0.03 | 2.22 | 42.66 | 86.49 |
| | 5 | 36.07 | 4.97 | 0.02 | 2.71 | 41.84 | 85.61 |
| | 6 | 36.64 | 5.03 | 0.02 | 1.59 | 42.88 | 86.16 |

**table S3. Results of TGA analyses.**

| | Impact Glasses | | | Breccia Pieces | | |
|---|---|---|---|---|---|---|
| | 160713 (30°) | 160714 (30°) | 160715 (45°) | 160713 (30°) | 160714 (30°) | 160715 (45°) |
| Initial mass (mg) | 14.8954 | 25.5023 | 14.0491 | 12.0232 | 11.2297 | 26.9499 |
| Mass at 190 °C (mg) | 14.8358 | 25.4219 | 14.0001 | 11.9440 | 11.1499 | 26.7706 |
| Mass at 850 °C (mg) | 14.7480 | 25.2949 | 13.9360 | 11.7660 | 10.9640 | 26.1830 |
| Mass Loss: Initial to 190 °C (wt.%) | 0.40% | 0.32% | 0.35% | 0.66% | 0.71% | 0.67% |
| Mass Loss: 190 to 850 °C (wt.%) | 0.59% | 0.50% | 0.46% | 1.49% | 1.67% | 2.19% |
| Start of major mass loss event (°C) | 515 | 600 | 495 | 590 | 515 | 570 |
| End of major mass loss event (°C) | 750 | 730 | 730 | 740 | 740 | 740 |
| Mass loss during event (wt.%) | 0.18% | 0.14% | 0.17% | 0.47% | 0.74% | 1.18% |
| DSC minimum (°C) | 178 | 145 | 194 | 149 | 147 | 140 |
| Temperatures of other DTG peaks (°C) | 146 | 145<br>660<br>690 | 154<br>700 | 155<br>350<br>430<br>645<br>695 | 150<br>340<br>410<br>550<br>645<br>690 | 153<br>475<br>640*<br>695 |

*Shoulder in DTG peak.

**table S4. Results of FULLPAT modeling.**

*Using diffraction pattern from 5 to 70° 2θ:*

| **Material** | **Experiment** | **$F_{serp}$ (wt.%)** | **$F_{targ}$ (wt.%)** | **$F_{glass}$ (wt.%)** | **Total (wt.%)** | **Σ│Delta│$^{1/2}$ *** | **R factor†** |
|---|---|---|---|---|---|---|---|
| Impact glasses | 160713 | 0.3 | 85.3 | 7.1 | 92.7 | 248.2 | 0.026 |
| | 160714 | 0.7 | 88.2 | 7.6 | 96.5 | 241.1 | 0.024 |
| | 160715 | 2.7 | 100.0 | 0.0 | 102.7 | 274.4 | 0.035 |
| Breccia pieces | 160713 | 2.4 | 92.8 | 2.5 | 97.7 | 248.6 | 0.022 |
| | 160714 | 1.4 | 100.0 | 9.5 | 110.8 | 262.3 | 0.026 |
| | 160715 | 7.9 | 89.0 | 0.4 | 97.3 | 251.4 | 0.022 |

*Using diffraction pattern from 12 to 12.4° 2θ:*

| **Material** | **Experiment** | **$F_{serp}$ (wt.%)** | **$F_{targ}$ (wt.%)** | **$F_{glass}$ (wt.%)** | **Total (wt.%)** | **Σ│Delta│$^{1/2}$ *** | **R factor†** |
|---|---|---|---|---|---|---|---|
| Impact glasses | 160713 | 0.3 | 87.3 | 6.3 | 93.9 | 1.2 | 0.027 |
| | 160714 | 0.5 | 100.0 | 1.7 | 102.2 | 2.2 | 0.032 |
| | 160715 | 0.8 | 100.0 | 0.0 | 100.8 | 0.0 | 0.058 |
| Breccia pieces | 160713 | 1.5 | 100.0 | 3.9 | 105.4 | 2.8 | 0.072 |
| | 160714 | 3.5 | 100.0 | 14.9 | 118.4 | 2.9 | 0.109 |
| | 160715 | 5.2 | 100.0 | 15.1 | 120.3 | 4.3 | 0.232 |

*The values of Σ│Delta│$^{1/2}$ that remain after optimizing the fit between the summed library standards and the observed pattern.
†R factors assess the quality of the model fit. $R < 0.1$ indicates a good analysis.

**table S5. Summary of Beer-Lambert results.**

| | | 3550 cm$^{-1}$ | | | 1630 cm$^{-1}$ | | | 4500 cm$^{-1}$ | | |
|---|---|---|---|---|---|---|---|---|---|---|
| Sample | Spot | Abs | Peak max (cm$^{-1}$) | $H_2O_{tot}$ (ppm) | Abs | Peak max (cm$^{-1}$) | $H_2O_m$ (ppm) | Abs | Peak max (cm$^{-1}$) | OH (ppm) |
| 160713 FTIR B* | 10 | 0.044 | 3589 | 445 | 0.026 | 1627 | 361 | - | - | - |
| 160713 FTIR B | 6 | 0.035 | 3589 | 355 | 0.028 | 1627 | 386 | - | - | - |
| 160713 FTIR B | 3 | 0.019 | 3438 | 190 | 0.016 | 1621 | 215 | - | - | - |
| 160714 FTIR A† | 1.0 | 0.135 | 3589 | 1486 | 0.059 | 1632 | 883 | 0.002 | 4518 | 951 |
| 160714 FTIR A | 1.1 | 0.191 | 3589 | 2100 | 0.074 | 1634 | 1117 | 0.003 | 4501 | 1407 |
| 160714 FTIR A | 1.2 | 0.116 | 3589 | 1273 | 0.060 | 1632 | 900 | 0.001 | 4462 | 635 |
| 160714 FTIR A | 1.3 | 0.163 | 3589 | 1797 | 0.065 | 1632 | 978 | 0.002 | 4462 | 1165 |
| 160714 FTIR A | 1.4 | 0.075 | 3589 | 828 | 0.037 | 1634 | 558 | 0.002 | 4462 | 836 |
| 160714 FTIR A | 1.5 | 0.103 | 3589 | 1135 | 0.053 | 1632 | 797 | 0.002 | 4520 | 942 |
| 160714 FTIR A | 3.3 | 0.238 | 3574 | 1763 | 0.073 | 1630 | 736 | 0.005 | 4440 | 1460 |
| 160714 FTIR A | 3.5 | 0.285 | 3589 | 2112 | 0.106 | 1630 | 1076 | 0.004 | 4435 | 1314 |
| 160714 FTIR A | 3.6 | 0.289 | 3589 | 2140 | 0.112 | 1632 | 1137 | 0.002 | 4462 | 551 |
| 160715 FTIR D‡ | 0 | 0.873 | 3622 | 9330 | 0.528 | 1632 | 7698 | 0.003 | 4520 | 1445 |
| 160715 FTIR D | 29 | 0.794 | 3591 | 8491 | 0.420 | 1632 | 6117 | 0.004 | 4460 | 1682 |
| 160715 FTIR D | 27 | 0.513 | 3591 | 5489 | 0.276 | 1632 | 4019 | 0.003 | 4442 | 1479 |
| 160715 FTIR D | 28 | 0.468 | 3591 | 5006 | 0.230 | 1632 | 3354 | 0.003 | 4442 | 1420 |
| 160715 FTIR D | 26 | 0.360 | 3589 | 3848 | 0.149 | 1630 | 2172 | 0.003 | 4460 | 1457 |
| 160715 FTIR D | 25 | 0.847 | 3622 | 9053 | 0.477 | 1632 | 6955 | 0.004 | 4462 | 1775 |
| 160715 FTIR D | 24 | 0.585 | 3591 | 6257 | 0.311 | 1630 | 4537 | 0.003 | 4520 | 1355 |
| 160715 FTIR D | 23 | 0.503 | 3591 | 5372 | 0.251 | 1630 | 3665 | 0.004 | 4460 | 1647 |
| 160715 FTIR D | 22 | 0.448 | 3591 | 4790 | 0.200 | 1632 | 2917 | 0.003 | 4442 | 1588 |
| 160715 FTIR D | 21 | 0.231 | 3589 | 2473 | 0.098 | 1630 | 1425 | 0.002 | 4462 | 1112 |
| 160715 FTIR D | 20 | 0.212 | 3587 | 2269 | 0.070 | 1630 | 1015 | 0.003 | 4440 | 1250 |
| 160715 FTIR D | 18 | 0.351 | 3589 | 3750 | 0.121 | 1630 | 1765 | 0.003 | 4435 | 1609 |
| 160715 FTIR D | 17 | 0.585 | 3591 | 6255 | 0.279 | 1632 | 4060 | 0.005 | 4442 | 2399 |
| 160715 FTIR D | 16 | 0.683 | 3622 | 7300 | 0.404 | 1632 | 5885 | 0.003 | 4462 | 1520 |
| 160715 FTIR D | 15 | 0.490 | 3591 | 5235 | 0.239 | 1632 | 3486 | 0.003 | 4460 | 1463 |
| 160715 FTIR D | 14 | 0.458 | 3591 | 4898 | 0.215 | 1632 | 3132 | 0.005 | 4435 | 2179 |
| 160715 FTIR D | 5 | 0.340 | 3589 | 3640 | 0.136 | 1630 | 1982 | 0.004 | 4460 | 1681 |
| 160715 FTIR D | 13 | 0.286 | 3589 | 3062 | 0.122 | 1630 | 1772 | 0.002 | 4520 | 1118 |
| 160715 FTIR D | 12 | 0.215 | 3589 | 2298 | 0.099 | 1627 | 1444 | 0.002 | 4460 | 897 |
| 160715 FTIR D | 11 | 0.163 | 3589 | 1741 | 0.075 | 1627 | 1097 | 0.002 | 4520 | 913 |
| 160715 FTIR D | 10 | 0.224 | 3589 | 2392 | 0.095 | 1630 | 1391 | 0.002 | 4520 | 916 |
| 160715 FTIR D | 9 | 0.293 | 3591 | 3137 | 0.117 | 1630 | 1698 | 0.003 | 4442 | 1329 |
| 160715 FTIR D | 8 | 0.265 | 3589 | 2832 | 0.108 | 1630 | 1568 | 0.003 | 4460 | 1226 |
| 160715 FTIR D | 7 | 0.260 | 3593 | 2776 | 0.122 | 1630 | 1774 | 0.003 | 4462 | 1222 |
| 160715 FTIR D | 6 | 0.188 | 3589 | 2009 | 0.065 | 1630 | 954 | 0.003 | 4435 | 1556 |
| 160715 FTIR D | 1 | 0.147 | 3589 | 1568 | 0.062 | 1630 | 905 | 0.001 | 4520 | 690 |
| 160715 FTIR D | 2 | 0.168 | 3587 | 1794 | 0.079 | 1630 | 1154 | 0.003 | 4462 | 1230 |
| 160715 FTIR D | 4 | 0.141 | 3589 | 1511 | 0.066 | 1630 | 964 | 0.002 | 4462 | 947 |

*Sample thickness: 0.0102 cm; density: 2,346 g L$^{-1}$
†Sample thickness: 0.0093 cm; density: 2,348 g L$^{-1}$
‡Sample thickness: 0.0096 cm; density: 2,341 g L$^{-1}$

**table S6. Compositions of projectile, target, and impact products.**

| | | $Al_2O_3$ (wt.%) | CaO (wt.%) | $FeO_T$ (wt.%) | $K_2O$ (wt.%) | MgO (wt.%) | MnO (wt.%) | $Na_2O$ (wt.%) | $SiO_2$ (wt.%) | Total (wt.%) |
|---|---|---|---|---|---|---|---|---|---|---|
| Antigorite projectile | Replicate 1 | 2.99 | 2.78 | 8.30 | 0.00 | 34.16 | 0.12 | 0.01 | 38.68 | 87.05 |
| | Replicate 2 | 2.99 | 2.70 | 8.17 | 0.03 | 33.91 | 0.12 | 0.02 | 39.31 | 87.25 |
| Heat-treated pumice target | Replicate 1 | 12.89 | 0.74 | 1.14 | 4.50 | 0.06 | 0.05 | 3.96 | 78.16 | 101.5 |
| | Replicate 2 | 12.88 | 0.64 | 1.15 | 4.45 | 0.06 | 0.05 | 4.05 | 77.34 | 100.6 |
| | Replicate 3 | 12.74 | 0.53 | 1.16 | 4.83 | 0.06 | 0.05 | 3.97 | 77.22 | 100.6 |
| | Replicate 4 | 12.63 | 0.51 | 1.11 | 4.79 | 0.06 | 0.05 | 4.09 | 78.23 | 101.5 |
| | | | | *Experiments* | | | | | | |
| 160713 (30°) | Glasses | 11.87 | 0.76 | 1.42 | 4.06 | 1.50 | 0.05 | 3.80 | 71.22 | 94.67 |
| | Breccias | 11.84 | 0.78 | 1.59 | 4.09 | 2.85 | 0.05 | 3.59 | 72.85 | 97.65 |
| 160714 (30°) | Glasses | 12.43 | 0.70 | 1.40 | 4.36 | 2.01 | 0.05 | 3.87 | 76.26 | 101.1 |
| | Breccias | 11.96 | 0.67 | 1.54 | 4.15 | 3.17 | 0.05 | 3.71 | 74.68 | 99.92 |
| 160715 (45°) | Glasses | 12.14 | 0.72 | 1.29 | 4.34 | 1.16 | 0.05 | 3.68 | 73.55 | 96.92 |
| | Breccias | 11.46 | 0.72 | 1.87 | 3.97 | 4.26 | 0.05 | 3.50 | 76.80 | 102.6 |

**table S7. Projectile retention efficiencies.**

| Experiment number | Angle (°) | Impact product | $X_{Serp}$ | $R^2$ | Fraction of projectile retained in material | 2σ |
|---|---|---|---|---|---|---|
| 160713 | 30 | Impact glasses | 0.071 | 0.993 | 6.2% | 0.6% |
| | | Breccias | 0.063 | 0.992 | 7.3% | 0.6% |
| | | Serpentine fragments | 1 | N/A | 2.4% | - |
| | | *Total retention* | | | *16%* | *1.1%* |
| 160714 | 30 | Impact glasses | 0.041 | 0.995 | 4.0% | 0.4% |
| | | Breccias | 0.052 | 0.977 | 6.5% | 0.9% |
| | | Serpentine fragments | 1 | N/A | 3.1% | - |
| | | *Total retention* | | | *14%* | *1.1%* |
| 160715 | 45 | Impact glasses | 0.034 | 0.975 | 3.2% | 0.6% |
| | | Breccias | 0.067 | 0.978 | 7.5% | 1.1% |
| | | Serpentine fragments | 1 | N/A | 7.9% | - |
| | | *Total retention* | | | *19%* | *1.2%* |